ANFIS modelling of mean gap voltage variation to predict wire breakages during wire EDM of Inconel 718

Abhilash P. M.*, D. Chakradhar

Department of Mechanical Engineering, Indian Institute of Technology Palakkad, Kerala, India, 678557

*Corresponding author: abhilashpm184@gmail.com, ORCID ID: 0000-0001-5655-6196

Abstract

The study aims to correlate the mean gap voltage variation and wire breakage occurrences during the wire EDM of Inconel 718. A novel approach to predict the wire breakage is introduced by considering the mean gap voltage variation (ΔV_m) as an indicator of the instabilities in the spark gap. Such instabilities are regarded as the primary reason for wire breakages and inferior part quality of wire electric discharge machined components. The parameter ΔV_m is a process data obtained as the difference between servo voltage and mean gap voltage (V_m). It was found experimentally that if the value of ΔV_m crosses a threshold limit, the process interruptions through wire breakages were observed. In order to predict the wire breakage situations, the study models ΔV_m using adaptive neuro fuzzy inference system (ANFIS). Based on central composite design (CCD) of response surface methodology (RSM), 31 experiments were conducted and ΔV_m is recorded as the response. The input parameters considered were pulse on time, pulse off time, servo voltage and wire feed rate. The ANFIS model was found very accurate in predicting ΔV_m, based on which wire breakage alerts can be given. The capability of the model is further confirmed by verification experiments. EDS and microstructural analysis further revealed the effect of ΔV_m on wire wear and part quality. Higher value of ΔV_m resulted in greater wire wear and inferior part quality. The surface finish and flatness error of machined parts were measured to compare the part quality.

Keywords *Wire electric discharge machining. ANFIS. Mean gap voltage. Wire breakage. Inconel 718*

This is a peer-reviewed, accepted author manuscript of the following article: P.M., A., & Chakradhar, D. (2020). ANFIS modelling of mean gap voltage variation to predict wire breakages during wire EDM of Inconel 718. CIRP Journal of Manufacturing Science and Technology, 31, 153-164. https://doi.org/10.1016/j.cirpj.2020.10.007

Nomenclature

V_m	Mean gap voltage
WEDM	Wire electric discharge machining
ΔV_m	Mean gap voltage variation
$\Delta V_{m,lim}$	Mean gap voltage variation limit
CCD	Central composite design
RSM	Response surface methodology
ANFIS	Adaptive neuro fuzzy inference system
SV	Servo voltage
WF	Wire feed rate
SEM	Scanning electron microscopy
EDS	Energy dispersive X-ray spectroscopy

1. Introduction

Wire electric discharge machining (WEDM) is a non-traditional manufacturing process which uses controlled and repetitive sparks for material removal [1]. The process is capable of machining any electrically conductive material with great accuracy. Since the tool, which is an electrically conductive wire, does not come into contact with the workpiece, the hardness of the workpiece does not limit the machinability. Therefore, the process is able to machine the hardest of the materials like superalloys and Ti alloys with ease [2]. However, the process is really stochastic since the sparks are generated between workpiece and wire at various random locations. Various process instabilities arise due to such stochastic nature of the process leading to surface defects and wire breakages. Debris accumulation, debris removal, dielectric flushing and many other factors contributes to the machining instabilities. Process interruptions by wire breakages makes the process unsustainable by increasing the machining time, energy utilization and material consumption. Even though it is relevant to study the process interruptions associated with the WEDM process to make the process sustainable, it is still not completely explored by the researchers.

Wire breakage detection due to instability was attempted by a few researchers in the past. Cabanes et al. [3] had attempted to detect wire breakages due to instability by setting up an acquisition system. The wire breakage scenarios were found to be depended on ignition delay time, peak current and pulse energy. Caggiano et al. [4] proposed feature extraction methods for various quality features which can determine the quality of machining process. The methodology involved getting the critical features from current and voltage sensor data by setting thresholds or by defining algorithms. Klocke et al. [5] researched on the relation between inter electrode gap and the machined surface quality. The voltage between the electrode was found to be an indicator of the spark gap which in turn effects the surface roughness. For controlling the surface roughness, they found that it is good enough to control the mean gap voltage. Tosun et al. [6] investigated the effects of process parameters on the crater sizes in wire electrode. The investigation was performed considering the crater diameter and depth as responses.

Bufardi et al. [7] had come up with an online fuzzy logic model to detect surface defects and recast layer during the wire electric discharge machining process. This is combined with an offline fuzzy logic model to handle surface roughness and recast layer thickness. The offline model aids in the initial input parameter settings and online model detects the defects in real time. Yan and Liao [8] developed a fuzzy logic-based model to prevent wire ruptures during wire-EDM. The model detects the sparking frequency in real-time and adjusts the pulse off time to reduce the frequency to safe limits. Lin et al. [9] had come up with a fuzzy logic-based control strategy to improve machining accuracy at corners. The model improved the corner machining accuracy by 50% by consuming only 10% extra machining time. Liao and Woo [10] developed a fuzzy based adaptive control system for the wire EDM process. The power consumption and short circuit ratio is monitored in real time. If the power consumption is more than a threshold value, the feed is

adjusted and if short circuit ratio is more pulse off time is increased to keep the machining stable. The feed and pulse off time are further fine-tuned according to ignition delay time.

Modelling the wire EDM responses using ANFIS was attempted by a few researchers in the past. Caydas et al., [11] developed an ANFIS model to predict white layer thickness and surface roughness. The model predictions were reported to be accurate when compared with experimental results. Azhiri et al. [12] modelled cutting seed and surface roughness by ANFIS for dry machining of Al/SiC metal matrix composite. Kumar et al. [13] applied ANFIS to model surface roughness and MRR during wire EDM of Ti- 6Al- 4V. Thee predicted responses showed good agreement with the experimental values with a minimum mean percentage error.

From the literature survey, it was understood that even though many Artificial Intelligence (A I) based soft computing tools were used to predict response characteristics, a wire breakage prediction system based on the mean gap voltage variation is yet to be attempted by the researchers. Such a model is of high significance to ensure the uninterrupted machining with high part accuracy. The current study sets a threshold limit for ΔV_m experimentally. An ANFIS model is trained using the RSM based experimental data considering ΔV_m as the response. The trained model predicts ΔV_m for any given input parameter settings, based on which wire breakages are forecasted.

1.1 Mean gap voltage variation

Mean gap voltage variation (ΔV_m) is the difference between the set value of gap voltage and the actual mean gap voltage during the process. When the machining conditions are optimal, the mean gap voltage (V_m) is expected to be stable with little variations [5]. However, due to the process mechanism which involves spark erosions and debris production, dielectric conductivity in the spark gap changes continuously and therefore V_m is observed to deviate from the set value. Varying amounts of suspended debris in the spark gap is the chief cause of the gap voltage

fluctuations. Higher variations imply a higher accumulation of debris and this can eventually result in wire breakages by spark gap bridging.

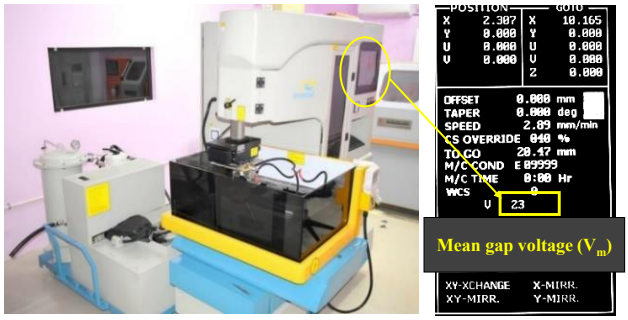

Fig. 1 (a) Machine tool (b) Integrated computer displaying mean gap voltage

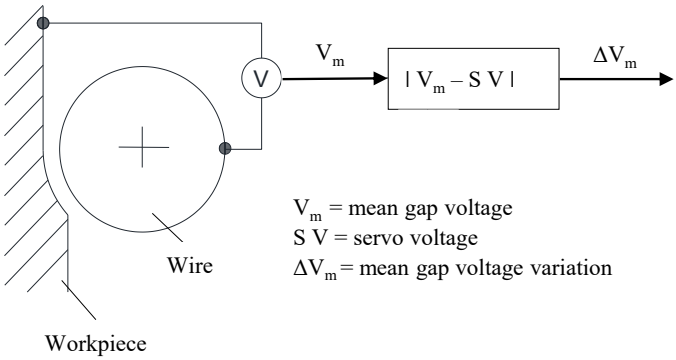

Fig. 2 Method of determining mean gap voltage variation

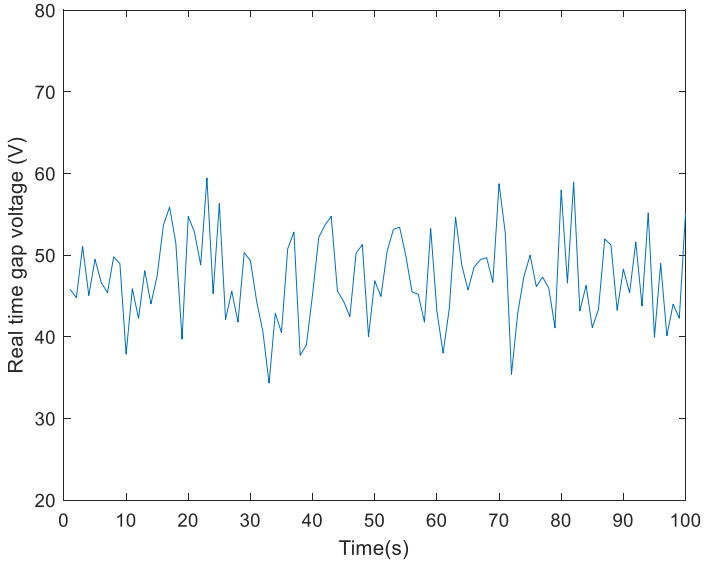

Fig. 3 Real-time gap voltage reading for a set voltage of 50 V

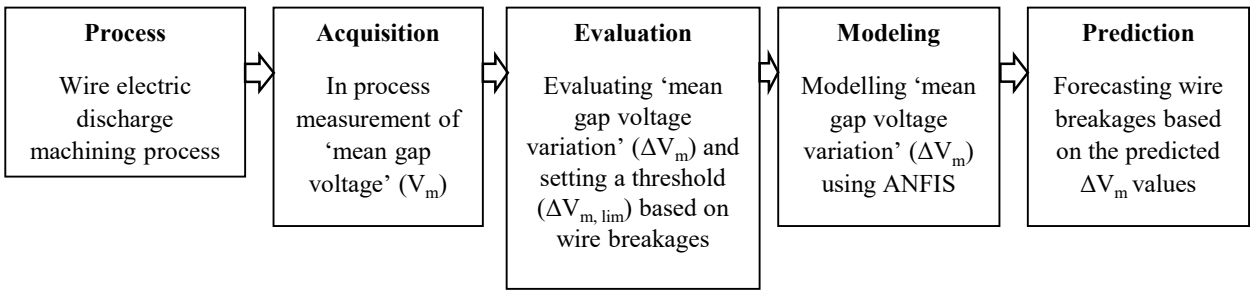

Fig. 4 Approach for predicting wire breakage

2. Materials and Methods

Experiments were conducted in a CNC controlled electronica ECOCUT wire electric discharge machine having a resolution of 1 µm. The profile was designed using ELCAM software which also generates the NC codes for the profile. Dielectric medium used was de-ionized water having a conductivity of 20 µS/cm. The wire electrode chosen was hard zinc coated brass wire of 0.25 mm diameter. Field emission scanning electron microscope (FESEM) Zeiss GeminiSEM 300 was used to analyze worn wire samples. The mean gap voltage (V_m) readings is displayed in the integrated computer as shown in Fig. 1. Fig. 2 shows the method of determining ΔV_m. The real-time reading of the gap voltage for a set voltage value of 50V is recorded using a Tektronix DAQ6510 digital multimeter and is shown in Fig. 3. The approach for predicting wire breakage occurrences are given in Fig. 4. Accurate Tutor 5.5.4 coordinate measuring machine (CMM) with a 3 mm diameter ruby probe was used to measure the flatness error. Zeiss Surfcom Flex 35-B contact type surface profilometer was used to measure the average surface roughness value. Cutoff length (L_c) and evaluation length was chosen as 0.8 mm and 4 mm respectively.

2.1 Workpiece material

Inconel 718 is chosen as the workpiece material due to its significance in high temperature applications. It is one of the Ni based superalloys which are prominently used for making turbine

components because of its ability to maintain the mechanical properties even at high temperatures. Since the material is considered difficult to machine conventionally, non-traditional machining processes like WEDM are relevant. The mechanical properties of Inconel 718 are given in Table 1. Table 2 shows the elemental composition for this material. The workpiece thickness was 10 mm and the machined profiles are all straight cuts.

Table 1 Properties of Inconel 718

Property	**Value**
Density	8.19 g/cm^3
Melting Point	1260 – 1336 ºC
Specific Heat	435 J/kg K
Average Coefficient of thermal expansion	13 µm/m K
Thermal Conductivity	11.4 W/m K
Ultimate Tensile strength	1240 MPa

Table 2 Chemical composition of Inconel 718

Element	**Ni**	**Fe**	**Cr**	**Nb**	**Mn**	**C**	**Co**	**Al**	**Si**	**Ti**	**Mo**	**Others**
Weight (%)	51.05	19.43	18.70	5.7	0.07	0.04	0.2	0.56	0.08	1.01	3.1	0.06

2.2 Experimental plan

The input parameters considered for the experimental analysis are pulse on time (T_{on}), Pulse off time (T_{off}), servo voltage (V) and wire feed rate (WF). In this work, wire tension and discharge current were kept constant due to WED machine constraints. The responses measured are the occurrence of wire breakages and mean gap voltage variation (ΔV_m). The experiments were conducted according to central composite design (CCD) of response surface methodology (RSM). The range of process parameters were selected based on pilot experiments and the machine specifications. The extreme ranges were selected purposely since the objective is to study and predict the wire breakages. Overall, thirty-one experiments were conducted and each experimental

run was repeated thrice. The ranges and levels for input parameters are given in Table 3. The parameters which are kept constant is given in Table 4.

Table 3 RSM input parameters and levels

Process parameters	Level 1	Level 2	Level 3	Level 4	Level 5
	Axial point (High)	Cube point (High)	Centre point	Cube point (Low)	Axial point (Low)
Pulse on Time (μs)	120	115	110	105	100
Pulse off Time (μs)	70	60	50	40	30
Servo voltage (V)	70	60	50	40	30
Wire feed rate (m/min)	10	8	6	4	2

Table 4. Constant machining parameters

Parameter	**Value**
Wire electrode diameter	0.25 mm
Discharge current	11 A
Discharge voltage	12 V
Flushing pressure	1.96 bar
Wire Tension	10 N
Dielectric fluid	Deionized water

3. Adaptive Neuro Fuzzy Inference System (ANFIS)

The adaptive neuro fuzzy inference system (ANFIS), proposed by Jang [14] combines the reasoning of artificial neural networks and fuzzy system. The system is computationally efficient and is suitable for modelling non-linear systems. ANFIS finds the optimum distribution of membership functions by a hybrid learning approach. The framework combining fuzzy and ANN makes the model more methodical and less dependent on expert knowledge. The architecture of

ANFIS has five layers as shown in Fig. 5. Each layer has several nodes defined by the node function. ANFIS uses a Takaki- sugeno type if-then rules to represent input output relationships.

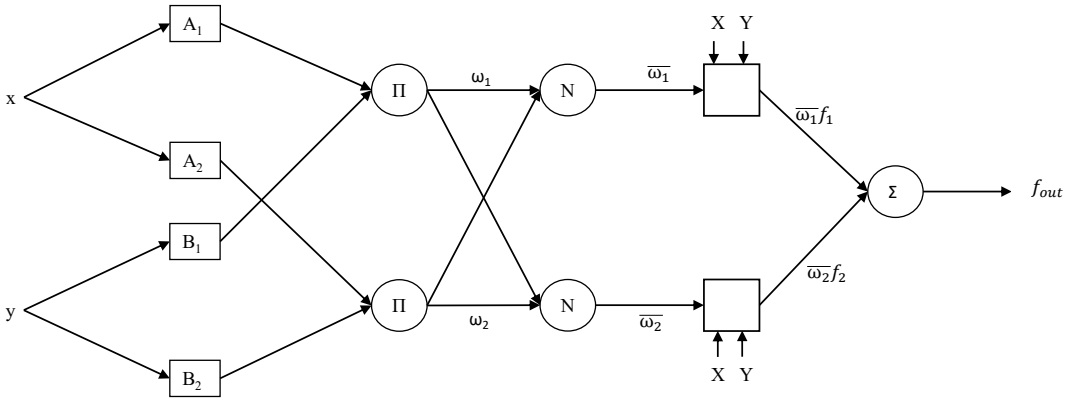

Fig. 5 ANFIS structure

The various steps in ANFIS are:

- ***Layer 1:*** The node function of first layer is defined as

$$O_{1,i} = \mu_{A_i}(x)\ for\ i = 1,2 \tag{1}$$

$$O_{1,i} = \mu_{B_{i-2}}(y)\ for\ i = 3,4 \tag{2}$$

where *x* and *y* are input parameters, A and B are linguistic labels of each input parameters. μ*(x)* and μ*(y)* are membership functions which are commonly triangular or bell shaped. In case of a triangular membership function, the function equation is

$$\mu(x) = \begin{cases} 0, & x \le a \\ \frac{x-a_i}{b_i-a_i}, & a \le x \le b \\ \frac{c_i-x}{c_i-b_i}, & b \le x \le c \\ 0, & c \le x \end{cases} \tag{3}$$

Otherwise, if the membership function is bell shaped (gaussian), the equation is

$$\mu(x) = exp\left(\frac{-(C_i-x)^2}{a_i^2}\right) \tag{4}$$

where $a_i, b_i \; and \; c_i$ are the parameters, based on which the shape of the respective membership function vary.

- ***Layer 2:*** In layer 2, all nodes are fixed nodes, labelled ⊓. The output function is the product of input signals given by

$$O_{2,i} = \omega_i = \mu_{A_i}(x) \,.\, \mu_{B_i}(y) \quad for\ i = 1, 2 \tag{5}$$

here the output ω_i denotes the rule's firing strength.

- ***Layer 3:*** The nodes are fixed nodes in this layer and are labelled N. The node function is to normalize the input signals.

$$O_{3,i} = \overline{\omega_i} = \frac{\omega_i}{\sum \omega_i} = \frac{\omega_i}{\omega_1 + \omega_2} \quad for\ i = 1, 2 \tag{6}$$

- ***Layer 4:*** The nodes of this layer are adaptive nodes with the following node function

$$O_{4,i} = \overline{\omega_i} \,.\, f_i \quad for\ i = 1, 2 \tag{7}$$

where $f_1 \; and \; f_2$ are fuzzy if-then rules defined by:

  - *Rule 1:* if x is A_1 and y is B_1 then $f_1 = p_1x + q_1y + r_1$
  - *Rule 2:* if x is A_2 and y is B_2 then $f_2 = p_2x + q_2y + r_2$

  where $p_i, \; q_i \; and \; r_i$ are called consequent parameters

- ***Layer 5:*** Nodes in this layer are fixed nodes, with the node function giving the overall output by the following equation

$$O_{5,i} = f_{out} = \sum_i \overline{w_i} \,.\, f_i \quad for\ i = 1, 2 \tag{8}$$

In ANFIS, the parameters are updated by a hybrid learning algorithm which is a combination of least squares and gradient descent algorithm. The parameters of the layer 4, the consequent parameters, are set by least squares estimate during the forward pass. On the other hand, the membership function parameters are set during back propagation by minimizing the error signals by gradient descent algorithm.

4. Results and Discussion

According to CCD design of RSM, 31 experiments were conducted. The response measured is wire breakage occurrence and mean gap voltage variation (ΔV_m) as given in Table 5. The profile machined was a straight rough cut of length 10 mm. To relate wire breakage occurrence with the mean gap voltage variation, the responses are plotted as shown in Fig. 6. Least value of ΔV_m corresponding to the first occurrence of wire breakage is considered as the threshold. The threshold value, $\Delta V_{m,\,lim}$ was fund to be $10.4^{+0.4}_{-0.2}\ V$. Every experimental run with $\Delta V_m \geq \Delta V_{m,\,lim}$ resulted in wire breakage. Every other case ($\Delta V_m < \Delta V_{m,\,lim}$) recorded a continuous straight rough cut. Higher variation in mean gap voltage implies greater instabilities in spark gap which resulted in wire breakage. For each wire electrode, workpiece, dielectric combinations, the threshold value will vary.

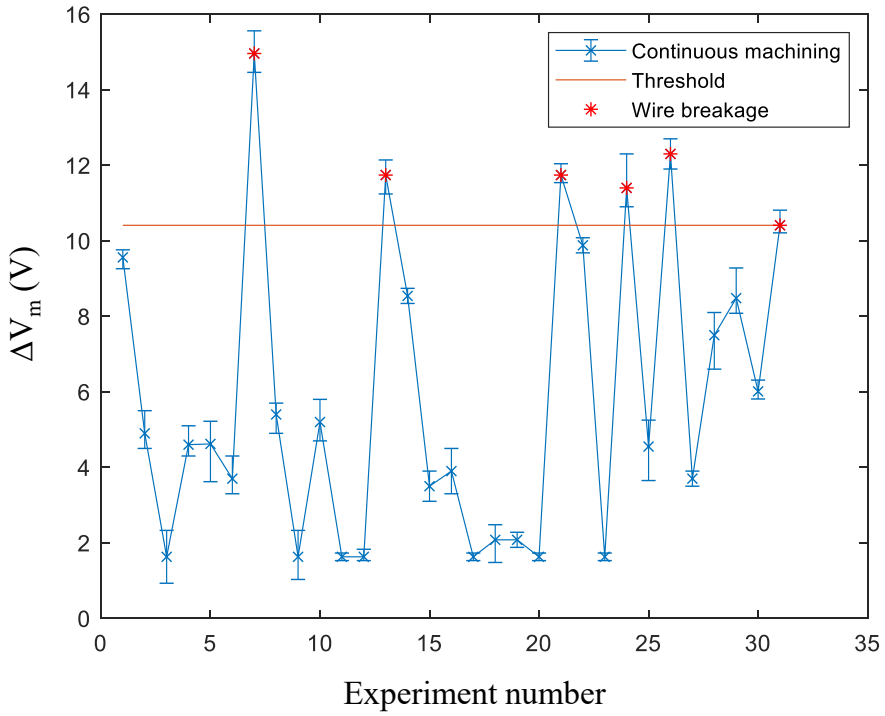

Fig. 6 Determination of mean gap voltage variation limit ($\Delta V_{m,\,lim}$)

Table 5 Experimental readings and model predictions

S. No.	Ton (µs)	Toff (µs)	SV (V)	WF (m/min)	Experimental readings			Model predictions	Error
					Wire breakage	Mean ΔV_m(V)	Std. Dev.	$\Delta V_{m.}$ (V)	(V)
1	115	40	60	4	0	9.56	0.2	9.56	0
2	110	50	50	6	0	4.9	0.4	4.67	0.23
3	105	60	60	4	0	1.63	0.6	1.63	0
4	110	50	50	6	0	4.6	0.4	4.67	-0.07
5	110	50	50	2	0	4.62	0.7	4.62	0
6	105	40	40	8	0	3.7	0.4	3.7	0
7	120	50	50	6	1	14.96	0.5	15	-0.04
8	110	50	50	10	0	5.4	0.4	5.4	0
9	100	50	50	6	0	1.63	0.5	1.63	0
10	110	50	50	6	0	5.2	0.5	4.67	0.53
11	105	60	60	8	0	1.63	0.1	1.63	0
12	105	60	40	8	0	1.63	0.1	1.63	0
13	115	40	40	4	1	11.74	0.4	11.7	0.04
14	115	40	60	8	0	8.54	0.2	8.54	0
15	110	50	50	6	0	3.5	0.3	4.67	-1.17
16	110	50	50	6	0	3.9	0.5	4.67	-0.77
17	105	40	60	8	0	1.63	0.1	1.63	0
18	110	50	70	6	0	2.08	0.5	2.08	0
19	110	70	50	6	0	2.08	0.1	2.08	0
20	105	60	40	4	0	1.63	0.1	1.63	0
21	115	40	40	8	1	11.74	0.2	11.7	0.04
22	115	60	60	4	0	9.88	0.2	9.88	0
23	105	40	60	4	0	1.63	0.1	1.63	0
24	115	60	40	4	1	11.4	0.6	11.4	0
25	110	50	50	6	0	4.55	0.6	4.67	-0.12
26	110	30	50	6	1	12.3	0.3	12.3	0
27	105	40	40	4	0	3.7	0.2	3.7	0
28	110	50	30	6	0	7.5	0.6	7.5	0
29	115	60	40	8	0	8.48	0.6	8.48	0
30	110	50	50	6	0	6.01	0.2	4.67	1.34
31	115	60	60	8	1	10.41	0.3	10.4	0.01

4.1 ANFIS model results

The experimental data is used to develop an ANFIS model. Table 5 compares the ANFIS model predictions with the experimental values of responses. Table 6 gives the model training parameters. Training input data set is a 31 x 4 matrix containing 31 combinations (according to CCD of RSM)

of four input parameters (T_{on}, T_{off}, SV and WF). Input membership function is gaussian in shape with a constant output function. Learning algorithm is hybrid combining both least squares and gradient descent algorithm. Table 7 shows the input Gaussian membership function parameters specified in equation (4). Similarly, Table 8 shows the consequent parameters of output membership function.

Table 6 ANFIS training parameters

Layers	5
Data set	31 x 4
Responses	1
Membership function	Gaussian
Learning algorithm	Least squares, gradient descent
Number of epochs	300
Output function	Constant

Table 7 Parameters of gaussian membership function

Factors	Low		Med		High	
	a	c	a	c	a	c
T_{on}	4.25	100	4.25	110	4.25	120
T_{off}	8.5	30	8.5	50	8.5	70
SV	8.5	30	8.5	50	8.5	70
WF	1.7	2	1.7	6	1.7	10

Table 8 Consequent parameters of output membership function

Exp. No.	Consequent parameters r_i	Exp. No.	Consequent parameters r_i
1	9.56	17	1.63
2	4.67	18	2.08
3	1.63	19	2.08
4	4.67	20	1.63
5	4.62	21	11.7
6	3.7	22	9.88
7	15	23	1.63
8	5.4	24	11.4
9	1.63	25	4.67
10	4.67	26	12.3
11	1.63	27	3.7
12	1.63	28	7.5
13	11.7	29	8.48
14	8.54	30	4.67
15	4.67	31	10.4
16	4.67		

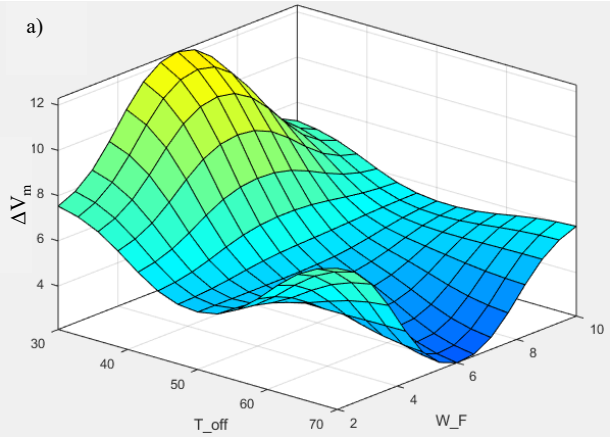

ΔV_m vs. Pulse off time and wire feed rate

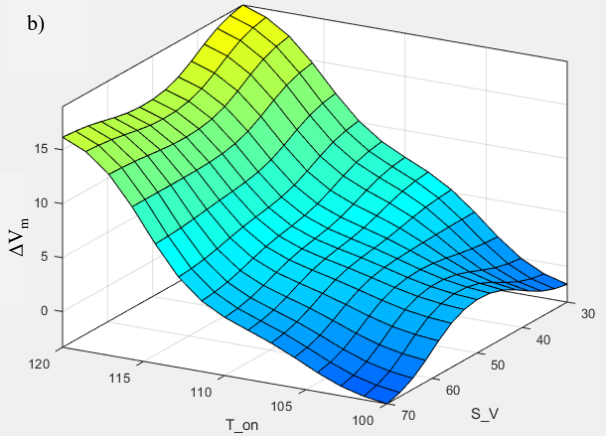

ΔV_m vs. Pulse on time and servo voltage

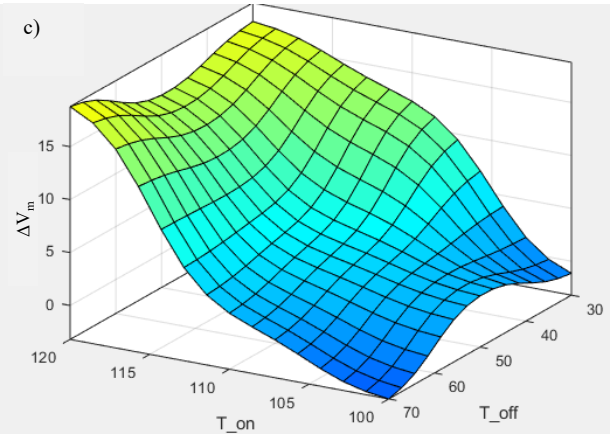

ΔV_m vs. Pulse on time and Pulse off time

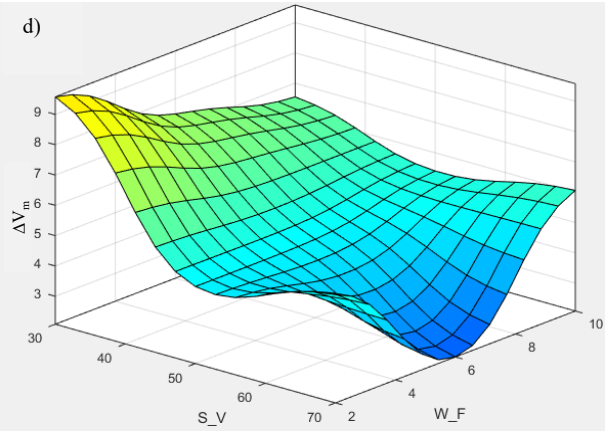

ΔV_m vs. Servo voltage and wire feed rate

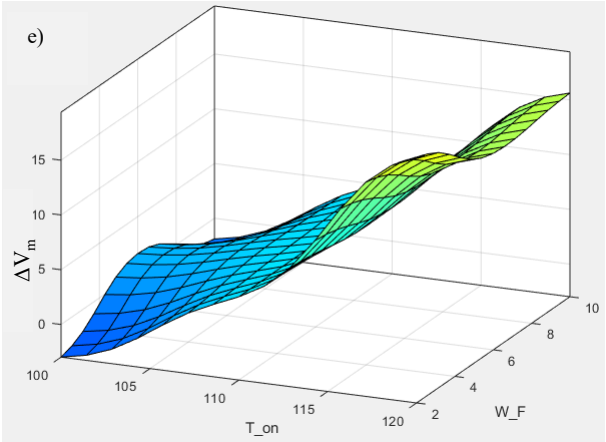

ΔV_m vs. Pulse on time and wire feed rate

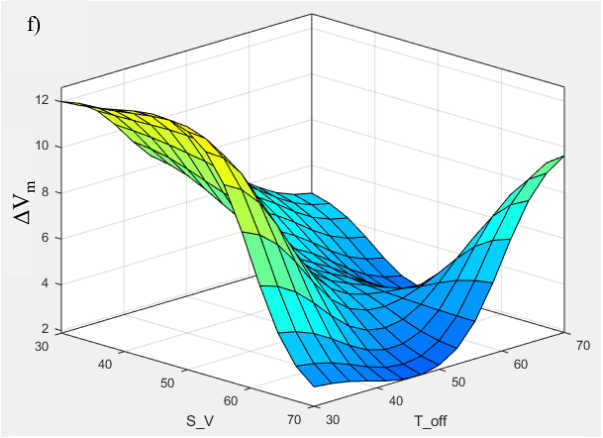

ΔV_m vs. Servo voltage and Pulse off time

Fig. 7 Surface plots showing the influence of process parameters on ΔV_m

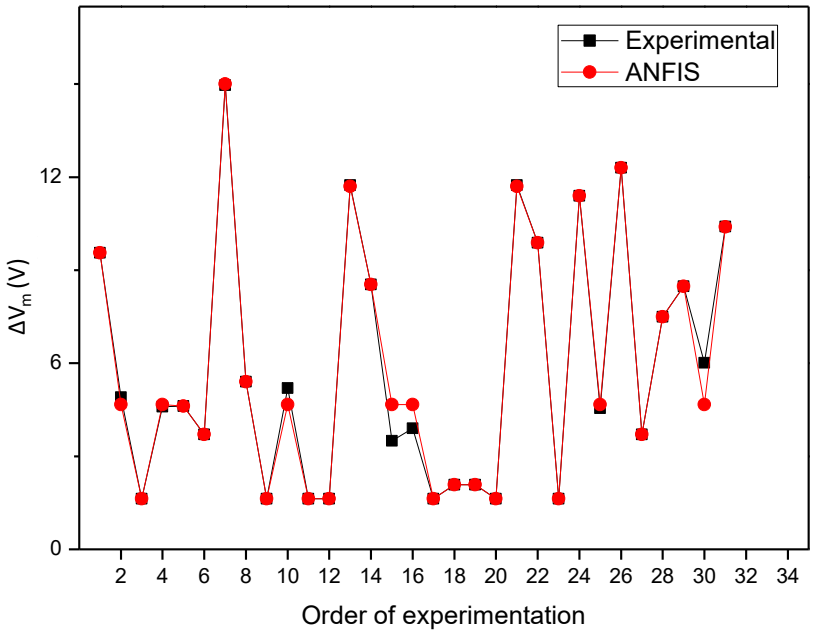

Fig. 8 Comparison of predicted values with actual values for ΔV_m

Fig. 7 shows the surface plots of ΔV_m obtained through ANFIS. Fig. 8 shows the comparison between the ANFIS predictions and experimental values for ΔV_m. The comparison with experimental values shows that the model gives an accurate prediction of response with only a marginal error. The predicted values coincide with the actual responses in most of the cases.

4.2 Human computer interaction - Wire break alert

A user interface is coded around the ANFIS model to interact with the operator. The interface gets the values of input parameter settings from the user and inputs them to the ANFIS model. The model processes the data and predicts the appropriate response, i.e., ΔV_m value. Based on this value, the interface suitably intimates the user whether to continue with the selected parameters or not. In case of ΔV_m crossing the threshold, a wire break alert is sent to the user, requesting a different parameter setting. The logic flow diagram of this interface is given below in Fig. 9. Table 10 shows the user interface for two cases from confirmation tests.

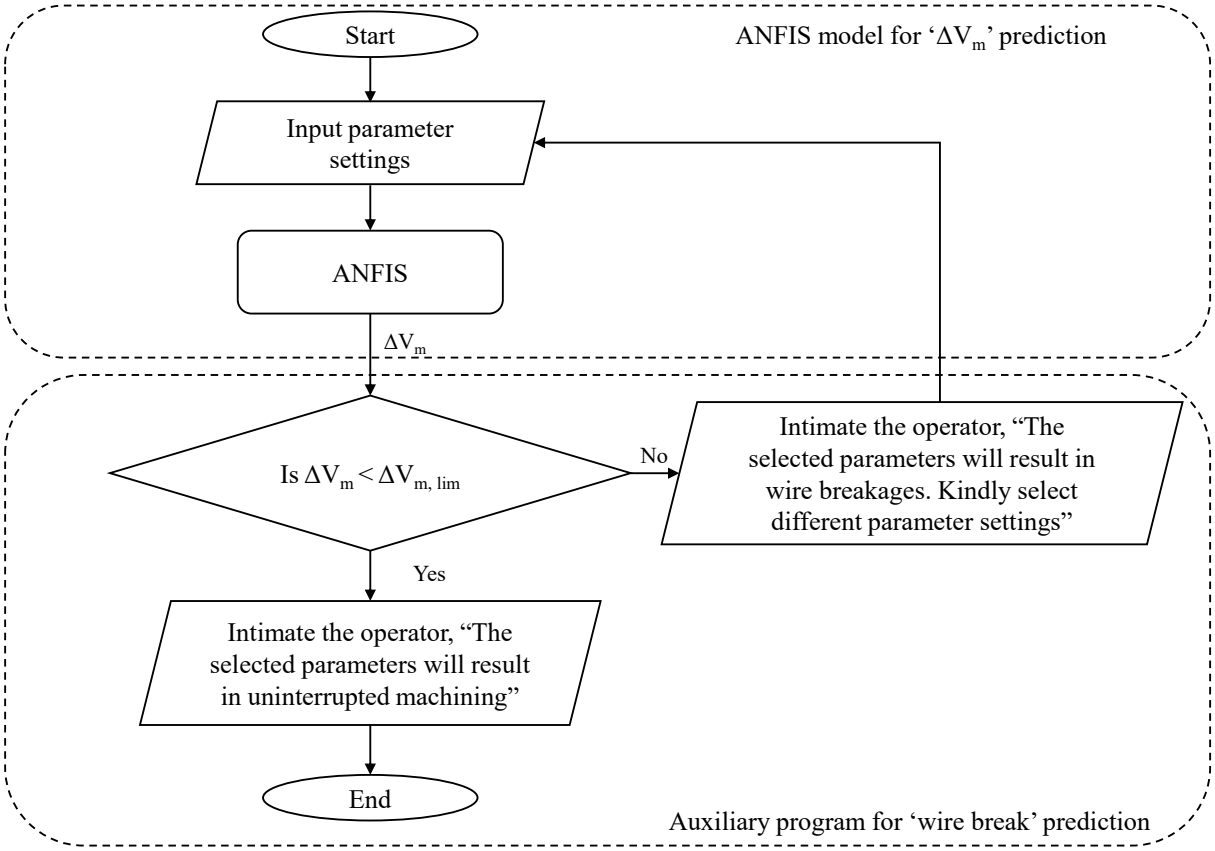

Fig. 9 Logic flow diagram for wire break alert

4.3 Confirmation experiments

Table 9 shows the results of the confirmation experiments. Whenever the predicted response was greater than $\Delta V_{m,\ lim}$, the wire breakages were observed. Also, the model predicted the response ΔV_m accurately with minimum errors. Fig. 10 shows the comparison between the experimental values and ANFIS predictions of ΔV_m for confirmation experiments.

Table 9 Confirmation experiments

S. No.	Ton (µs)	Toff (µs)	SV (V)	WF (m/min)	ANFIS ΔV_m	Exp. ΔV_m	Model prediction	Experimental observation
1	115	40	30	3	9.79	8.8	CM	CM
2	115	30	40	3	8.57	8.4	CM	CM
3	120	30	30	7	14.5	15.2	WB	WB
4	120	30	40	4	12	10.8	WB	WB
5	105	45	40	5	3.28	3.5	CM	CM
6	110	35	40	10	7.91	8.05	CM	CM
7	118	33	39	4	11.8	12	WB	WB
8	112	43	49	9	7.33	7.25	CM	CM
9	103	33	31	5	2.77	2.5	CM	CM

CM – Continuous machining, WB – wire breakage

Table 10. Wire break intimation based on ANFIS model predictions

Experiment number	**Model input**	**Model output - wire breakage prediction**
Experiment number 03	Pulse on time = 120 µs Pulse off time = 30 µs Servo voltage = 30 V Wire feed rate = 7 m/min	Mean gap voltage variation = 14.5 V 'Gap voltage variation will lead to wire breakages. Kindly select different input parameter settings'
Experiment number 05	Pulse on time = 105 µs Pulse off time = 45 µs Servo voltage = 40 V Wire feed rate = 5 m/min	Mean gap voltage variation = 3.28 V 'Selected input parameter settings will result in uninterrupted machining'

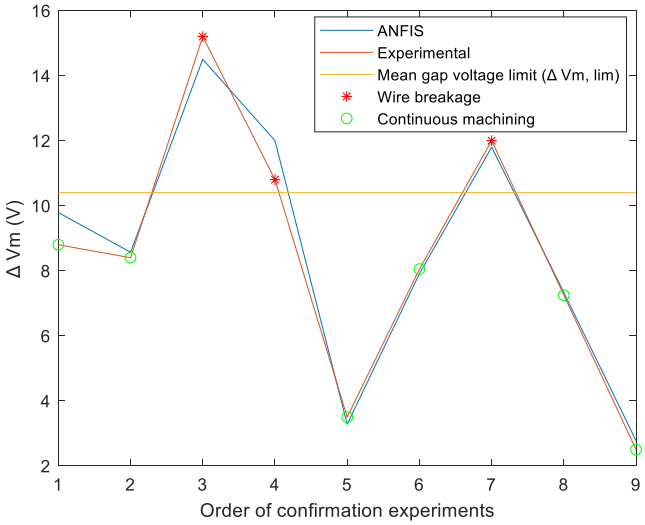

Fig. 10 Confirmation tests comparison of ANFIS responses with experimental readings

4.4 Surface Integrity Analysis

4.4.1 Microstructural Examination

The model predictions were categorised into low, medium and high as shown in Table 11. The worn wire samples belonging to each of the three categories were analysed under SEM. As shown in Fig. 11, SEM images of wire surface shows that the wire wear increases as ΔV_m increases, ultimately leading to the wire rupture. This is because, high ΔV_m implies a greater gap instability resulting in debris accumulation and short circuit discharges. These higher discharge energy sparks are considered unwanted/ harmful sparks and thus can lead to excessive wire wear. When the zinc coatings are worn off the inner brass core is exposed leading to wire breakage. Limit at which the wire is unable to withstand the gap instabilities is given by $\Delta V_{m,\,lim}$ value. Fig. 11 (c to e) shows broken wire tip images of all the wire breakage cases during confirmation tests.

Apart from causing higher wire wear, gap instabilities deteriorate part quality too. This is studied by considering SEM images of machined surfaces at each of the above three categories. Fig. 12 shows the SEM images of machined parts at different predicted ΔV_m values. Also surface

roughness, and flatness error were compared to understand part quality differences at different levels of ΔV_m.

Table 11 Classification of mean gap voltage variation

Predicted ΔV_m	Category
< 5	Low
5 to 10	Medium
>10	High

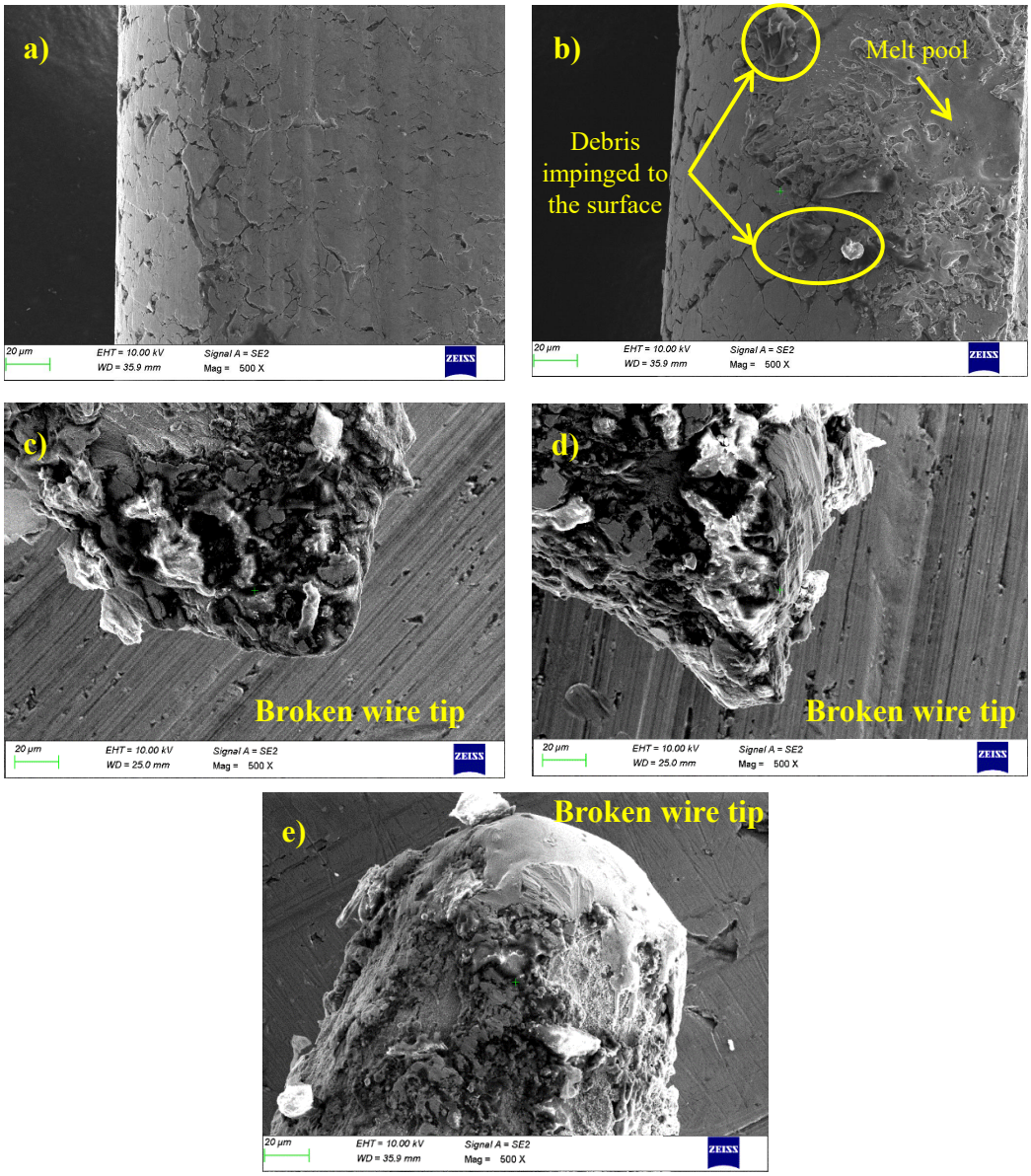

Fig. 11 SEM images of wire surfaces with (a) low ΔV_m (b) medium ΔV_m (c) broken wire tip at high ΔV_m (Exp. No. 3) (d) broken wire tip (Exp. No. 4) (e) broken wire tip (Exp. No. 7)

Table 12 shows the comparison of part quality for confirmation experiments. It is observed that the experimental runs with higher ΔV_m predictions produced surfaces with greater roughness and flatness deviations. Flatness error was measured using acute tutor make coordinate measuring machine (CMM). The flatness error helps to learn the effect of ΔV_m on the geometric errors. Geometric errors are caused by wire vibrations. As mentioned in previous section ΔV_m is an indicator of gap stability. Higher ΔV_m indicates higher instability resulting in greater unbalanced lateral forces causing wire vibrations. Due to this effect flatness error improved at low ΔV_m predictions. Surface roughness is higher for higher ΔV_m since such machining conditions are associated with higher energy short circuit sparks which causes surface damages or irregularities.

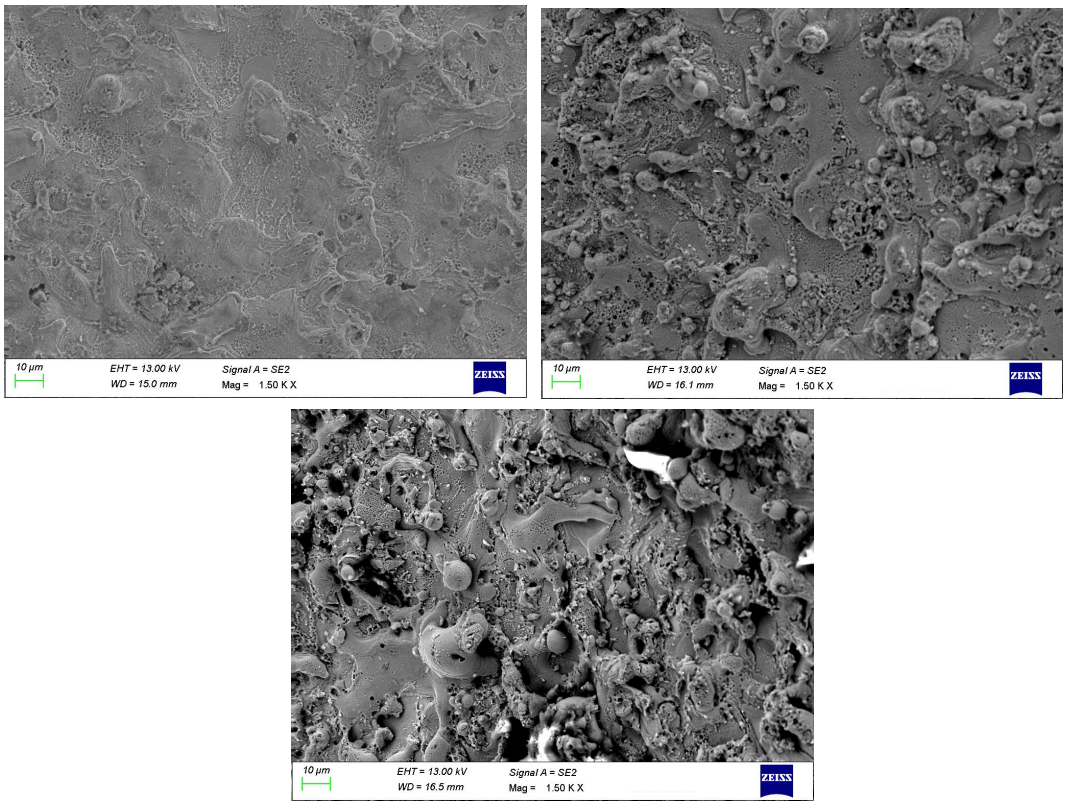

Fig. 12 SEM images of machined surfaces with (a) low ΔV_m (b) medium ΔV_m (c) high ΔV_m prediction

Table 12 Part quality comparison at different ΔV_m predictions

S. No.	ΔV_m (V) ANFIS	ΔV_m (V) Experimental	Surface Roughness R_a (μm)	Flatness Error FE (μm)	Wire breakage
1	9.79	8.8	3.54	4.75	No
2	8.57	8.4	3.22	4.01	No
3	14.5	15.2	-	-	Yes
4	12	10.8	-	-	Yes
5	3.28	3.5	1.9	1.21	No
6	7.91	8.05	3.1	3.23	No
7	11.8	12	-	-	Yes
8	7.33	7.25	2.83	2.61	No
9	2.77	2.5	1.4	0.9	No

4.4.2 EDS of worn wire electrodes at different instabilities

Energy dispersive spectroscopy (EDS) was performed on the worn wire samples to analyse the effect ΔV_m on compositional differences. When the sample surface is exposed to electron beam, characteristic x-rays are emitted back. These x-rays are captured and measured for the elemental analysis. The analysis gives the weight percentage of each elements from a small area of the surface. Fig. 13 shows the EDS spectrum of wire surfaces under low, medium and high ΔV_m predictions. Higher ΔV_m indicates an unstable machining condition, which is primarily caused by debris accumulation in the spark gap. Since these accumulated debris are not effectively flushed away, they tend to bridge the narrow spark gap between the wire electrode and workpiece. This situation leads to the formation of unwanted arc or short circuit discharges between the two electrodes. These types of discharges are associated with extremely high discharge energies which results in higher wire wear. The zinc coated wire electrodes are normally preferred over uncoated electrodes due to its better overall performance. The coatings are reported to protect the inner wire core from thermal shock. This zinc coating will be rapidly removed from the wire electrode surface by the action of these short circuit sparks. The zinc wt. % was less in the first case due to the

extensive zinc coting removal. On the other hand, lower value of ΔVm indicates a stable machining with lesser debris accumulation. In such situations, the normal discharge sparks dominate the pulse cycle which has comparatively lesser discharge energy. Due to the lesser spark energy, the extend of zinc coating is removal is less. The EDS analysis also support this argument. From the EDS images it can be observed that, zinc wt. % decreases from case (a) to (c) due to greater zinc coating removal from the wire surface.

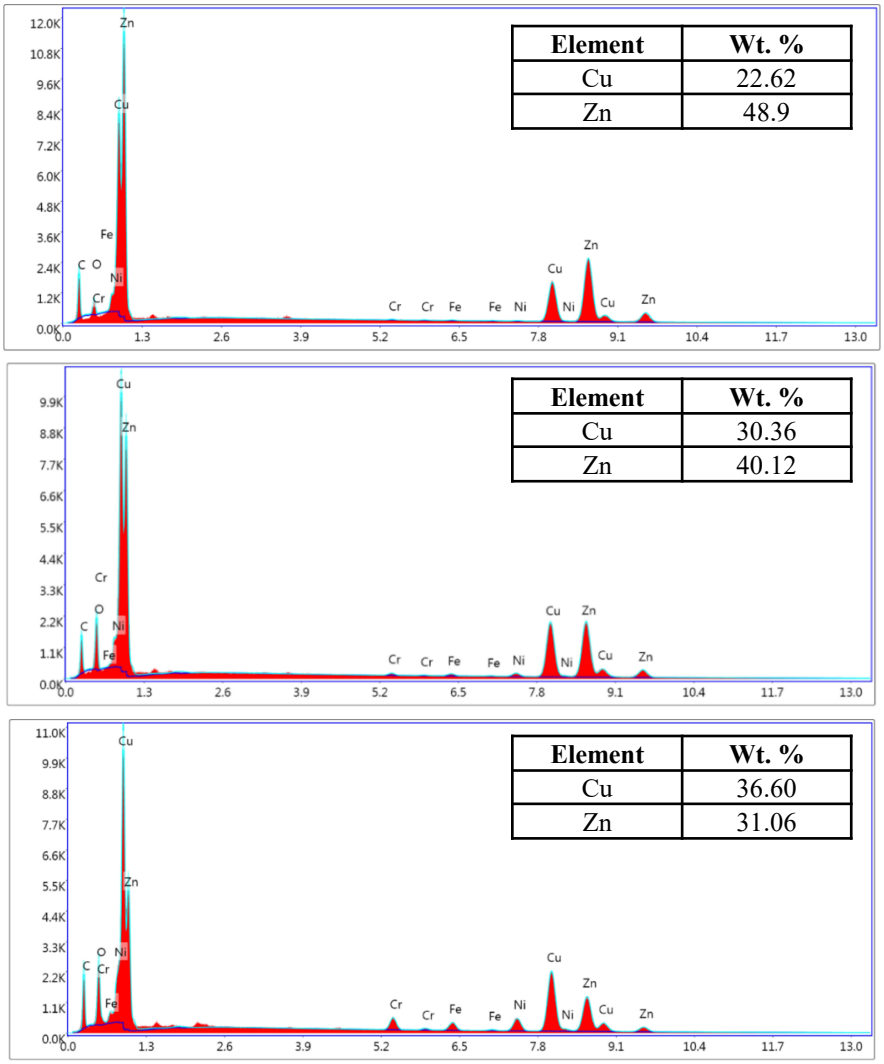

Fig. 13 EDS analysis of wire surfaces with (a) low ΔV_m (b) medium ΔV_m (c) high ΔV_m prediction

5. Conclusions

The mean gap voltage variation of wire electric discharge machining process was modelled using ANFIS. This model handles the uncertainties and randomness associated with the machining process and predict the instabilities accurately. Following are the salient conclusions from the study

1. The threshold value of ΔV_m, which is the upper limit for continuous and uninterrupted machining during the wire EDM of Inconel 718, was found experimentally.
2. The response ΔV_m was modelled using ANFIS and the model was found to be accurate in its wire breakages prediction.
3. Confirmation tests proved the capacity of the model to predict ΔV_m. Based on this, suitable alerts can be given regarding the wire breakages. Whenever the predicted ΔV_m values were greater than the threshold limit, wire breakages were observed.
4. Higher wire wear was observed at high ΔV_m compared to low ΔV_m predictions when SEM images of wire samples are compared. Wire breakage has occurred due to significant deterioration of wire surface causing catastrophic failure. Similarly, greater surface damages were observed at higher ΔV_m predictions. At high ΔV_m, R_a and flatness errors were observed to be more.
5. Elemental analysis showed lesser zinc contents at higher ΔV_m proving higher degradation of wire coatings.

Acknowledgement

The authors would like to acknowledge the central instrumentation facility, Indian Institute of Technology Palakkad for providing the test facilities.

Funding

This research did not receive any specific grant from funding agencies in the public, commercial, or not-for-profit sectors.

References

[1] Ho KH, Newman ST, Rahimifard S, Allen RD. State of the art in wire electrical discharge machining (WEDM). Int J Mach Tools Manuf 2004; 44:1247–59.

[2] Mandal A, Dixit AR. State of art in wire electrical discharge machining process and performance. Int J Mach Mach Mater 2014; 16:1.

[3] Cabanes I, Portillo E, Marcos M, Sánchez JA. An industrial application for on-line detection of instability and wire breakage in wire EDM. J Mater Process Technol 2008; 195:101–9.

[4] Caggiano A, Teti R, Perez R, Xirouchakis P. Wire EDM monitoring for zero-defect manufacturing based on advanced sensor signal processing. Procedia CIRP 2015; 33:315–20.

[5] Klocke F, Welling D, Klink A, Perez R. Quality assessment through in-process monitoring of wire-EDM for fir tree slot production. New Prod Technol Aerosp Ind - 5th Mach Innov Conf (MIC 2014)-Procedia CIRP 2014; 24:97–102.

[6] Tosun N, Cogun C, Pihtili H. The Effect of Cutting Parameters on Wire Crater Sizes in Wire EDM. Int J Adv Manuf Technol 2003; 21:857–65.

[7] Bufardi A, Akten O, Arif M, Xirouchakis P. Towards zero-defect manufacturing with a combined online - offline fuzzy-nets approach in wire electrical discharge machining 2017:401–9.

[8] Yan MT, Liao YS. A self-learning Fuzzy controller for wire rupture prevention in WEDM. Int J Adv Manuf Technol 1996; 11:267–75.

[9] Lin C-T, Chung I-F, Huang S-Y. Improvement of machining accuracy by fuzzy logic at corner parts for wire-EDM. Fuzzy Sets Syst 2001; 122:499–511.

[10] Liao YS, Woo JC. Design of a fuzzy controller for the adaptive control of WEDM process. Int J Mach Tools Manuf 2000; 40:2293–307.

[11] Çaydaş U, Hasçalik A, Ekici S. An adaptive neuro-fuzzy inference system (ANFIS) model for wire-EDM. Expert Syst Appl 2009; 36:6135–9.

[12] Azhiri B, Teimouri R, Ghasemi Baboly M, Leseman Z. Application of Taguchi, ANFIS and grey relational analysis for studying, modeling and optimization of wire EDM process while using gaseous media. Int J Adv Manuf Technol 2014; 71:279–95.

[13] Kumar S, Dhanabalan S, Narayanan CS. Application of ANFIS and GRA for multi-objective optimization of optimal wire-EDM parameters while machining Ti–6Al–4V alloy. SN Appl Sci 2019; 1:1–12.

[14] Jang J. R. ANFIS: adaptive-network-based fuzzy inference system. IEEE Trans Syst Man Cybern 1993, 23(3), 665–685